Article

Effect of the Phase States of Self-Assembled Monolayers on Pentacene Growth and Thin-Film Transistor Characteristics

Hwa Sung Lee, Do Hwan Kim, Jeong Ho Cho, Minkyu Hwang, Yunseok Jang, and Kilwon Cho

J. Am. Chem. Soc., **2008**, 130 (32), 10556-10564 • DOI: 10.1021/ja800142t • Publication Date (Web): 17 July 2008

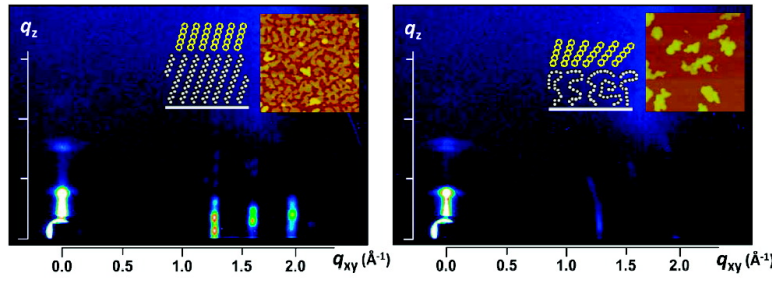

More About This Article

Additional resources and features associated with this article are available within the HTML version:

- Supporting Information
- Access to high resolution figures
- Links to articles and content related to this article
- Copyright permission to reproduce figures and/or text from this article

View the Full Text HTML

J|A|C|S
ARTICLES

Published on Web 07/17/2008

Effect of the Phase States of Self-Assembled Monolayers on Pentacene Growth and Thin-Film Transistor Characteristics

Hwa Sung Lee, Do Hwan Kim, Jeong Ho Cho, Minkyu Hwang, Yunseok Jang, and Kilwon Cho*

Department of Chemical Engineering/Polymer Research Institute, Pohang University of Science and Technology, Pohang, 790-784, Korea

Received January 8, 2008; E-mail: kwcho@postech.ac.kr

Abstract: To investigate the effects of the phase state (ordered or disordered) of self-assembled monolayers (SAMs) on the growth mode of pentacene films and the performance of organic thin-film transistors (OTFTs), we deposited pentacene molecules on SAMs of octadecyltrichlorosilane (ODTS) with different alkyl-chain orientations at various substrate temperatures (30, 60, and 90 °C). We found that the SAM phase state played an important role in both cases. Pentacene films grown on relatively highly ordered SAMs were found to have a higher crystallinity and a better interconnectivity between the pentacene domains, which directly serves to enhance the field-effect mobility, than those grown on disordered SAMs. Furthermore, the differences in crystallinity and field-effect mobility between pentacene films grown on ordered and disordered substrates increased with increasing substrate temperature. These results can be possibly explained by (1) a quasi-epitaxy growth of the pentacene film on the ordered ODTS monolayer and (2) the temperature-dependent alkyl chain mobility of the ODTS monolayers.

Introduction

Pentacene is one of the most promising organic semiconductors for use as the active material in organic thin-film transistors (OTFTs) because of its high mobility, which is comparable to that of amorphous silicon.[1–5] The device performance of pentacene TFTs is dramatically influenced by the structural order within the pentacene layer such as the packing morphology and the molecular interactions.[6,7] Particularly the structural order near the dielectric/active layer[8–11] and the electrode/active layer interfaces[11,12] plays a critical role in determining the device performances, because charge transport in OTFTs take places within several monolayers near the interface of the gate dielectrics. This structural order is in turn highly sensitive to the substrate characteristics (surface energy,[13,14] roughness,[8,15] and surface molecular structures[7,16]) of gate dielectrics because the interactions between the pentacene molecules and the substrate surface determine how the molecules assemble in the vicinity of the surface, that is, in the first monolayer, over which the overlayers then grow.[17,18]

To study the effect of the gate dielectric/active layer interface, many researchers have used a variety of dielectric layers with different surface properties.[5,19–22] Self-assembled monolayers (SAMs) have been introduced in inorganic dielectrics to lower the surface energy, thereby affecting the morphology and structural order of pentacene.[23–25] Bao and co-workers reported a high field-effect mobility of 3.5 $cm^2/(V \cdot s)$, which was

(1) Dimitrakopoulos, C. D.; Purushothaman, S.; Kymissis, J.; Callegari, A.; Shaw, J. *Science* **1999**, *283*, 822.
(2) Babel, A.; Jenekhe, S. A. *Adv. Mater.* **2002**, *14*, 371.
(3) Horowitz, G. *Adv. Mater.* **1998**, *10*, 365.
(4) Shtein, M.; Mapel, J.; Benziger, J. B.; Forrest, S. R. *Appl. Phys. Lett.* **2002**, *81*, 268.
(5) Kobayashi, S.; Nishikawa, T.; Takenobu, T.; Mori, S.; Shimoda, T.; Mitani, T.; Shimotani, H.; Yoshimoto, N.; Ogawa, S.; Iwasa, Y. *Nat. Mater.* **2004**, *3*, 317.
(6) Fritz, S. E.; Martin, S. M.; Frisbie, C. D.; Ward, M. D.; Toney, M. F. *J. Am. Chem. Soc.* **2004**, *126*, 4084.
(7) Kim, C.; Facchetti, A.; Marks, T. J. *Science* **2007**, *318*, 76.
(8) Yang, H.; Shin, T. J.; Ling, M. -M.; Cho, K.; Ryu, C. Y.; Bao, Z. *J. Am. Chem. Soc.* **2005**, *127*, 11542.
(9) Chabinyc, M. L.; Salleo, A.; Endicott, F.; Ong, B. S.; Wu, Y.; Liu, P.; Heeney, M.; McCulloch, I. *Proc. SPIE* **2005**, *5940*, 594012.
(10) Halik, M.; Klauk, H.; Zschieschang, U.; Schmid, G.; Dehm, C.; Schütz, M.; Malsch, S.; Effenberger, F.; Brunnbauer, M.; Stellacci, F. *Nature* **2004**, *431*, 963.
(11) Zaumseil, J.; Sirringhaus, H. *Chem. Rev.* **2007**, *107*, 1296.
(12) Lee, H. S.; Cho, J. H.; Kim, W. -K.; Lee, J. -L.; Cho, K. *Electrochem. Solid-State Lett.* **2007**, *10*, H239.
(13) Dimitrakopoulos, C. D.; Malenfant, P. R. L. *Adv. Mater.* **2002**, *14*, 99.
(14) Ruiz, R.; Nickel, B.; Koch, N.; Feldman, L. C.; Haglund, R. F.; Kahn, A.; Scoles, G. *Phys. Rev. B* **2003**, *67*, 125406.
(15) Stadlober, B.; Haas, U.; Maresch, H.; Haase, A. *Phys. Rev. B* **2006**, *74*, 165302.
(16) Schiefer, S.; Huth, M.; Dobrinevski, A.; Nickel, B. *J. Am. Chem. Soc.* **2007**, *129*, 10316.
(17) Yanagisawa, H.; Tamaki, T.; Nakamura, M.; Kudo, K. *Thin Solid Films* **2004**, *464*, 398.
(18) Meyer zu Heringdorf, F.-J.; Reuter, M. C.; Tromp, R. M. *Nature* **2001**, *412*, 517.
(19) Pratontep, S.; Nüesch, F.; Zuppiroli, L.; Brinkmann, M. *Phys. Rev. B* **2005**, *72*, 085211.
(20) Ruiz, R.; Choudhary, D.; Nickel, B.; Toccoli, T.; Chang, K.-C.; Mayer, A. C.; Clancy, P.; Blckely, J. M.; Headrick, R. L.; Iannotta, S.; Malliaras, G. G. *Chem. Mater.* **2004**, *16*, 4497.
(21) Kline, R. J.; DeLongchamp, D. M.; Fischer, D. A.; Lin, E. K.; Heeney, M.; McCulloch, I.; Toney, M. F. *Appl. Phys. Lett.* **2007**, *90*, 062117.
(22) Schreiber, F. *Phys. Stat. Sol. A* **2004**, *201*, 1037.
(23) Lee, H. S.; Kim, D. H.; Cho, J. H.; Park, Y. D.; Kim, J. S.; Cho, K. *Adv. Funct. Mater.* **2006**, *16*, 1859.
(24) Lin, Y.-Y.; Cundlach, D. J.; Nelson, S. F.; Jackson, T. N. *IEEE Electron Device Lett.* **1997**, *18*, 87.

10.1021/ja800142t CCC: $40.75

achieved by introducing hexamethyldisilazane on silicon oxide dielectrics.[8] Iwasa and co-workers studied the effect of the surface energy on the electrical properties of pentacene TFTs by using various SAMs with different functional groups such as $-CF_3$, $-CH_3$, and $-NH_2$.[5,25] Among all SAM materials, octadecyltrichlorosilane (ODTS) has been widely used as an effective surface modifier because of the uniform and reproducible surface properties it affords.[13,24–27] The effects of treating the surface with ODTS on the pentacene structures and device performances were studied by Forrest, Whang, and others.[26–29] The studies mainly focused on the relationship between the electrical characteristics of the devices and changes in the grain size, molecular structure, and charge-carrier density of pentacene. However, the physical properties of the ODTS monolayers vary according to the preparation conditions, that is, preparation temperature, humidity, and substrate roughness, although the surface energy of the prepared SAMs is the same.[30–34] The phase states (ordered/disordered) of the ODTS monolayers are particularly influenced by the preparation temperature.[33,34] In the ODTS monolayers prepared below 30 °C, the alkyl chains are tightly packed, thus resulting in ordered monolayers. On the other hand, at preparation temperatures above 30 °C, the monolayers exhibit a disordered state, which is originated from the loose packing and higher mobility of the alkyl chains. Considering the deposition process of pentacene molecules onto a substrate, we can expect different interactions to occur between these molecules and the different phase states of the ODTS monolayer. Such interactions can affect the morphology and molecular order of the deposited pentacene layers. However, the effects of the phase states of SAMs on pentacene growth and device performance have been neglected up to now.

Here, we present an experimental study on the effects of the phase states of SAMs on both the growth of pentacene films and the electrical properties of TFTs based on such films. To achieve this goal, we used ODTS monolayers, in which the phase states of the alkyl chains can be controlled (ordered/disordered). Furthermore, we systematically varied the substrate temperature to study the temperature dependence of the crystallinity and the growth behavior of the pentacene film on the phase-state-controlled substrates. To analyze the structural and morphological characteristics of both the ODTS monolayers and the pentacene films, Fourier-transform infrared (FT-IR) and near-edge X-ray absorption fine structure spectroscopy (NEXAFS) studies, as well as X-ray diffraction (XRD) and atomic force microscopy (AFM) experiments, were performed. The relationship between these properties and the electrical performance of pentacene TFTs was also investigated.

Experimental Section

For the fabrication of the OTFTs, a highly doped p-Si wafer with a 300-nm thick thermally grown oxide layer was used as the substrate. The wafer serves as gate electrode while the oxide layer acts as gate insulator. Prior to the surface treatment of the silicon oxide layer, the wafer was cleaned in piranha solution (70 vol % H_2SO_4 + 30 vol % H_2O_2) for 30 min at 100 °C and washed with copious amounts of distilled water. As an organic interlayer between the organic active material and the dielectric layer, we used the coupling agent octadecyltrichlorosilane (ODTS, Gelest) as purchased. The self-assembled monolayers were prepared using a dipping method at different preparation temperatures. We deposited ODTS at 4 and 65 °C to fabricate ordered and disordered alkyl-chain structures of SAMs, respectively. The surface wettability of the prepared SAMs was determined by measuring the contact angle between a probe liquid (hexadecane) and the monolayer surface using a contact angle meter (Krüss BSA 10). The thickness of the SAMs was determined using an ellipsometer (M-2000V, J. A. Woollam Co., Inc.), and their root-mean-square (rms) roughness was examined by using atomic force microscopy (AFM, Digital Instruments Multimode). The chain conformation was investigated by means of FT-IR spectroscopy (Bruker IFS 66v), using p-polarized light with an incident angle of 80°, as well as by X-ray photoemission spectroscopy (XPS), and NEXAFS, with incident angles of 20 and 90° (2B1 and 4B1 beam lines at the Pohang Accelerator Laboratory, Korea).

Pentacene (organic semiconductor, Aldrich Chemicals, no purification) was deposited from a quartz crucible onto the ODTS-modified substrates at a rate of 0.2 Å/s by using an organic molecular-beam deposition (OMBD) system, keeping the temperature of the crucible close to 210 °C under a base pressure of approximately 10^{-7} Torr. The deposition rates (0.2 Å/s), film thickness, and substrate temperature were nominally recorded by the monitor. The devices were completed by evaporating gold through a shadow mask to define the source and drain contacts onto a 50-nm-thick pentacene film, forming the active layer of the OTFT. The channel length and width were fixed at 100 and 800 μm, respectively. To investigate the inner structure of the pentacene thin films, the X-ray diffraction (XRD) measurements were performed using the 3C2, 4C2, 8C1, and 10C1 beam lines (wavelength $\approx$ 1.54 Å) at the Pohang Accelerator Laboratory, Korea.

To study the current−voltage characteristics of the prepared devices, the OTFTs were operated in the accumulation mode by applying a negative gate bias. The source electrode was grounded and the drain electrode was negatively biased. All the results were obtained at room temperature under ambient conditions in a dark environment, using the Keithley 2400 and 236 source/measure units.

Results and Discussion

To confirm the physical structure (the degree of molecular ordering/molecular packing density) of the ODTS monolayers prepared at different temperatures (4 and 65 °C), we analyzed the spectra obtained in the FT-IR, NEXAFS, and XPS experiments. Figure 1a shows the FT-IR spectra of the ODTS monolayers. The bands at 2919 and 2850 cm^{-1} are assigned to the asymmetric and symmetric CH_2 stretching modes, respectively.[34–36] Characteristic IR peaks resulting from the methylene ($-CH_2-$) stretching vibrations of well-ordered monolayers were observed at about 2919 cm^{-1} for the ODTS monolayer deposited at 4 °C, whereas in the case of the monolayer deposited at 65 °C,

(25) Takeya, J.; Nishikawa, T.; Takenobu, T.; Kobayashi, S.; Iwasa, I.; Mitani, T.; Goldmann, C.; Krellner, C.; Batlogg, B. *Appl. Phys. Lett.* **2004**, *85*, 5078.
(26) Park, Y. D.; Lim, J. A.; Lee, H. S.; Cho, K. *Mater. Today* **2007**, *10*, 46.
(27) Shtein, M.; Mapel, J.; Benziger, J. B.; Forrest, S. R. *Appl. Phys. Lett.* **2002**, *81*, 268.
(28) Kang, S. J.; Yi, Y.; Kim, C. Y.; Whang, C. N.; Callcott, T. A.; Krochak, K.; Moewes, A.; Chang, G. S. *Appl. Phys. Lett.* **2005**, *86*, 232103.
(29) Knipp, D.; Street, R. A.; Volkel, A.; Ho, J. *J. Appl. Phys.* **2003**, *93*, 347.
(30) Leggett, G. J. *Anal. Chim. Acta* **2003**, *479*, 17.
(31) Onclin, S.; Ravoo, B. J.; Reinhoudt, D. N. *Angew. Chem., Int. Ed.* **2005**, *44*, 6282.
(32) Ulman, A. *Chem. Rev.* **1999**, *96*, 1533.
(33) Lee, D. H.; Oh, T.; Cho, K. *J. Phys. Chem. B* **2005**, *109*, 11301.
(34) Cho, J. H.; Lee, D. H.; Shin, H. S.; Pattanayek, S. K.; Ryu, C. Y.; Cho, K. *Langmuir* **2004**, *20*, 11499.
(35) Iimura, K.; Nakajima, Y.; Kato, T. *Thin Solid Films* **2000**, *379*, 230.
(36) Rye, R. R. *Langmuir* **1997**, *13*, 2588.

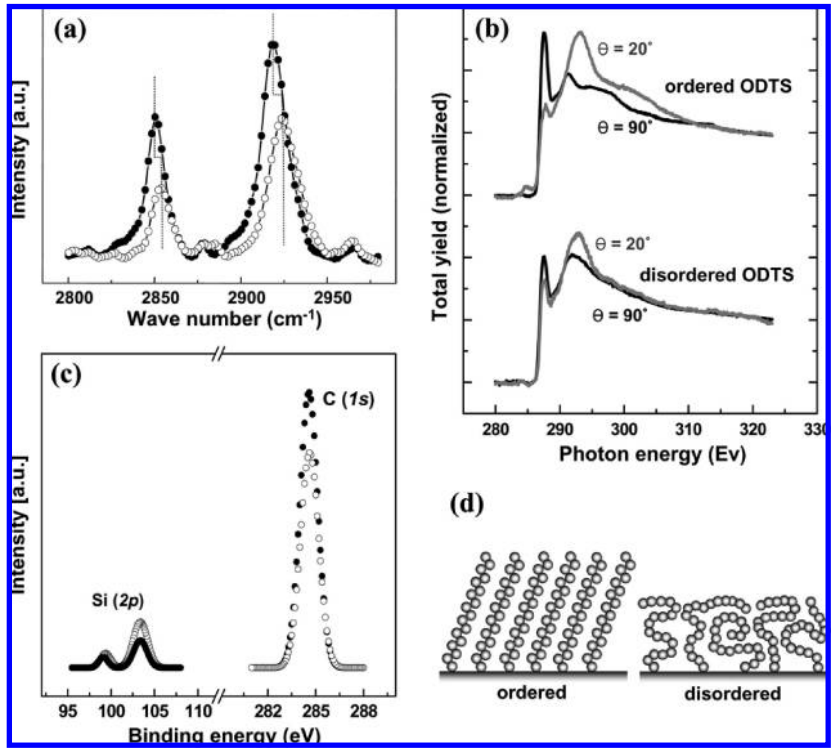

Figure 1. (a) Infrared external reflection spectra of ordered (closed symbols) and disordered (open symbols) ODTS monolayers on silicon. (b) High-resolution NEXAFS spectra of the C1s edge of ODTS monolayers on silicon (recorded at different angles of incidence, θ). (c) XPS results showing the C(1s) and Si(2p) binding-energy peaks of silicon substrates modified with ordered (closed symbols) and disordered (open symbols) ODTS monolayers. (d) Schematic representation of the ordered (left) and disordered (right) monolayers.

these characteristic peaks exhibited an upward shift. These results indicate that the ordered chain structures which contain a high portion of molecules in the trans conformation transform into disordered structures exhibiting increasing gauche defects.[34–36]

We confirmed the influence of the preparation temperature on the conformational changes of the ODTS monolayers by using both NEXAFS and IR spectroscopy. Figure 1b shows a series of NEXAFS spectra taken at room temperature for two different incident angles (namely, $\theta = 90$ and 20°). The spectra are dominated by two resonances, which originate from the C−H σ* and C−C σ* orbitals.[37–39] The sharp features situated at 287.9 eV originate from transitions into the C−H σ* orbitals. For the ordered ODTS monolayers, the intensity of the bands obtained using a normal X-ray incidence ($\theta = 90°$) is stronger than that observed with a grazing incidence ($\theta = 20°$). The broader resonance band found at around 293.3 eV can be assigned to transitions into the C−C σ* orbital.[37–39] The grazing-incidence intensity of this signal is stronger than its normal-incidence intensity. For the ordered ODTS monolayer, the transitions into the C−H σ* and C−C σ* orbitals show an opposite polarization dependence on the incident angles. This dependence is, however, weaker in this case of the disordered monolayer. The results indicate that most of the chains in the ordered ODTS monolayer are oriented perpendicularly to the surface, whereas those in the disordered ODTS monolayer are loosely oriented.[37–41]

We also carried out XPS experiments to evaluate the chain packing density in the ordered and disordered ODTS monolayers. Figure 1c shows the corresponding Si(2p) and C(1s) XPS spectra on an SiO_2 substrate. The XPS spectrum in the Si(2p) range shows two peaks at 99.5 and 103.5 eV, which are due to elemental silicon (Si^0) and SiO_2 (Si^{4+}), respectively.[42–44] The integrated area of these two peaks is smaller for the ordered ODTS monolayer than for the disordered one. A single C(1s) peak observed at 284.6 eV is consistent with a single alkane environment in the molecule, the integrated peak area for the ordered ODTS monolayer being larger than that for the disordered one. Discrepancies in the integrated peak areas of the Si(2p) and C(1s) signals for the ordered and disordered ODTS monolayers can be attributed to the different thicknesses of the monolayers on the SiO_2 substrates, namely, 24 Å for the ordered case and 16 Å for the disordered case (Table 1). The C(1s)/Si(2p) peak ratio was used as a measure of the relative chain packing density of the ODTS monolayers on the dielectrics (Table 1).[42–44] This ratio was found to be 38% larger in the ordered case than in the disordered one, which indicates a higher chain packing density for the ordered ODTS monolayers.

Based on AFM, contact-angle, ellipsometry, FT-IR, NEXAFS, and XPS results [Table 1 and Figure 1 a, b, and c], we can conclude that the alkyl chains of the ODTS monolayers prepared at 4 and 65 °C have molecularly different physical states (i.e., ordered and disordered orientations, respectively).

(37) Kim, D. H.; Jang, Y.; Park, Y. D.; Cho, K. *Langmuir* **2005**, *21*, 3203.
(38) Bagus, P. S.; Weiss, K.; Schertel, A.; Wö ll, Ch.; Braun, W.; Hellwig, C.; Jung, C. *Chem. Phys. Lett.* **1996**, *248*, 129.
(39) Weiss, K.; Bagus, P. S.; Wö ll, Ch. *J. Chem. Phys.* **1999**, *111*, 6834.
(40) Tourillon, G.; Fontaine, A.; Garrett, R.; Sagurton, M.; Xu, P.; Williams, G. P. *Phys. Rev. B* **1987**, *35*, 9863.
(41) Väterlein, P.; Schmelzer, M.; Taborski, J.; Krause, T.; Viczian, F.; Bässler, M.; Fink, R.; Umbach, E.; Wurth, W. *Surf. Sci.* **2000**, *452*, 20.
(42) Mirji, S. A. *Surf. Interface Anal.* **2006**, *38*, 158.
(43) Wang, Y.; Lieberman, M. *Langmuir* **2003**, *19*, 1159.
(44) Arias, A. C.; Endicott, F.; Street, R. A. *Adv. Mater.* **2006**, *18*, 2900.

Table 1. Characteristics of the Ordered and Disordered ODTS Monolayers Prepared on Gate Dielectrics

sample	thickness[a]. Å	surface energy[b]. mJ/m^2	rms roughness[c]. Å	C(1s)/Si(2p) ratio[d]
ordered ODTS	24	23.5	4.2	7.3
disordered ODTS	16	23.8	4.5	4.5

[a] Measured by ellipsometry. [b] Calculated from the hexadecane contact angles (ordered ODTS, 33°; disordered ODTS, 31°) using the equation of Good−Girifalco and Fowkes, $\gamma_{sv} = \gamma_{lv}(1 + \cos\theta)^2/4$.[32] [c] Measured by AFM. [d] Normalized with respect to the thickness of the ODTS monolayers.

However, both monolayers exhibit identical surface-energy and surface-roughness. The structures of the monolayers, which have different chain packing densities and different chain orientations, are schematically shown in Figure 1d).

To investigate crystalline phase and crystallinity of the deposited pentacene films, synchrotron XRD measurements were performed. The X-ray diffraction patterns of the $\theta-2\theta$ scans for 50 nm-thick pentacene films on the ordered and disordered ODTS monolayers at various substrate temperatures, namely, 30, 60, and 90 °C are shown in Figure 2a. The presence of only *(00l)* reflections indicates that all pentacene nanocrystals in the thin films are oriented with their *(00l)* planes parallel to the gate dielectric.[23,45] Furthermore, the typical XRD patterns of the pentacene thin films indicate the presence of two distinct crystalline polymorphs, referred to as the "thin-film" and "bulk" phases, which are characterized by different d_{001} spacings, namely, 15.5 ± 0.1 and 14.5 ± 0.1 Å, respectively.[23,45] As shown in Figure 2b,c, the pentacene films deposited on ordered ODTS monolayers were found to have higher peak intensities for both the "thin-film" and the "bulk" phases; this indicates an increased crystallinity of the pentacene films deposited on the ordered monolayer.[4,13] The higher peak intensity ratio of the thin-film phase to the bulk phase was observed in the ordered cases compared to the disordered cases. It indicates that the pentacene molecules deposited on the ordered ODTS monolayer would be more apparently affected by the interaction with the monolayer surface, because thin-film phase is a surface-induced phase (or strained phase) which is energetically less stable in comparison to the bulk phase.[46] Moreover, the intensity of the diffraction peaks increased with the substrate temperature in both cases; this increase was particularly significant for the pentacene film deposited on the ordered ODTS monolayer.

Figure 3 shows two-dimensional grazing-incidence X-ray diffraction (2D GIXD) patterns of 10 nm-thick pentacene films deposited on the ODTS monolayers at 30 °C. In the ordered case, intense *(00l)* crystal reflections, which can be used as a criterion for a thin-film phase, show at q_z direction satisfying Bragg's law, suggesting that most of the *(00l)* plane of pentacene crystals is oriented parallel to the substrate.[23,45] The 2D GIXD patterns also show three intense in-plane reflections of the thin-film phase appearing vertically at a given q_{xy} (> 0), which can be indexed to {1, ± 1}, {0, 2}, and {1, ± 2}, respectively.[8] The presence of these vertical "Bragg-rod" reflections indicates that the pentacene film on the ordered ODTS monolayer consists of well-multistacked layers. In addition, the weak reflection peaks marked with white arrows in Figure 3a are supposed to be those of "bulk phase" pentacene crystals. By contrast, in the disordered case, both *(00l)* and *(00l)′* crystal reflections are

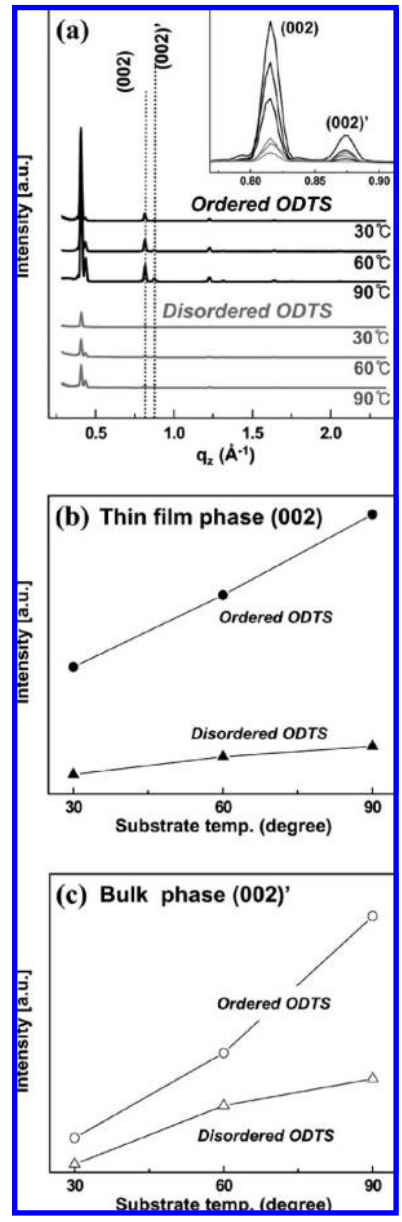

Figure 2. (a) X-ray diffraction patterns of the 50 nm-thick pentacene films deposited on ordered (top) and disordered (bottom) ODTS monolayers at 30, 60, and 90 °C. Relative intensities of the thin-film phase (002) (b) and the bulk phase (002)′ (c) of 50 nm-thick pentacene films as a function of the substrate temperature. The inset of panel a shows the enlarged (002) and (002)′ peaks of the XRD pattern.

shown at the q_z direction and are more scattered along the Debye rings. The in-plane reflections also show the highly scattered patterns along the Debye rings. These results indicate the pentacene film on the disordered ODTS monolayer has serious crystal mismatch and dislocation in the vertical and lateral directions.

To analyze crystal perfection in the films, we also analyzed the rocking curve (see Supporting Information Figure S2). The full width at half maximum (FWHM) of the physical rocking curves gives us the information about the perfection in crystal packing. That is, the rocking curve method is one way to evaluating crystallinity.[47,48] In result, the full width at half

(45) Mattheus, C. C.; de Wijs, G. A.; de Groot, R. A.; Palstra, T. T. M. *J. Am. Chem. Soc.* **2003**, *125*, 6323.
(46) Yoshida, H.; Inaba, K.; Sato, N. *Appl. Phys. Lett.* **2007**, *90*, 181930.
(47) J. Nogués, J.; Zakharchenko, I. V.; Rao, K. V. *Thin Solid Films* **1998**, *325*, 30.

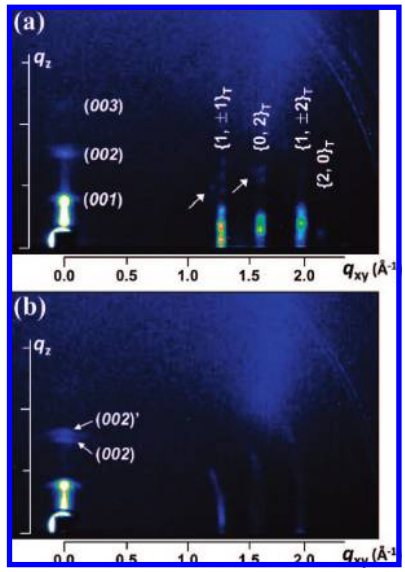

Figure 3. 2D GIXD patterns of the 10 nm-thick pentacene films deposited on ordered (a) and disordered (b) ODTS monolayers at 30 °C.

maximum (FWHM) at (002) peak along out-of-plane was found to be 56% larger in the disordered case than in the ordered one. It indicates higher crystal perfection in a pentacene film for the ordered case.

It is important to know how the self-ordering of pentacene admolecules affects the nucleation and film-growth mechanisms on the substrates. Therefore, we investigated the serial-growth processes of the pentacene islands. Figure 4 shows AFM images of pentacene films deposited on ordered and disordered ODTS monolayers at various substrate temperatures (namely, 30, 60, and 90 °C). Differences in the growth mechanisms are evident. In the case of the ordered ODTS monolayers [Figure 4a], numerous two-dimensional islands were formed during the initial stages of pentacene film growth. The step height of these islands was about 3.2−5.0 nm, which corresponds to a thickness of about 2−3 pentacene layers. As the thickness of the deposited pentacene continued to increase, the islands grew laterally and eventually coalesced. This predominant interconnection between the grains was observed at a nominal thickness of 30 Å. However, at nominal thicknesses above 100 Å, vertical growth of the islands was observed rather than lateral growth (Stranski−Krastanov mode).[49] The same growth behavior was observed at higher substrate temperatures, despite the larger grain size of pentacene (Figure 4a).

In the case of the disordered ODTS monolayers (Figure 4b), conglomerated island-type structures were formed on the substrate surface during the initial stages of the deposition process. With increasing nominal thickness, more structures of this kind appeared on the vacant regions and the grain size did not increase laterally. Furthermore, there was no vertical growth of the islands and no connection between the grains until a nominal thickness of 100 Å was reached, the height of the islands being about 15 nm (columnar growth mode).[49] This behavior also remained constant, even at higher substrate temperatures (Figure 4b). From these results, it can be expected that the pentacene films deposited on the ordered ODTS monolayers will be connected in several layer levels, which results in a better interconnectivity between the grains relative to that observed in the case of the disordered monolayers.[50–52]

Additionally, we briefly analyzed the surface kinetics of the pentacene molecules by investigating the nucleation density and the grain size in Figure 4. At the early stages of growth, the nucleation density (N) in the first seeding layer is known to be related to the ratio between the diffusion constant (D) and the deposition rate (F) by the following equation: $N \propto F/D$.[51,53] The value of D determines the average diffusion distance an admolecule has to travel before adsorbing to the surface. In our experiment, the value of F is fixed to 0.2 Å/s, which means that N is mainly determined by the value of D of the pentacene species adsorbed on the ODTS surfaces. This value seems to be smaller on the ordered surfaces than on the disordered ones, as suggested by the smaller number (and larger size) of nuclei formed on the disordered substrate. This result may be due to the greater mobility of the disordered (amorphous-like) ODTS surface. Furthermore, as the substrate temperature increases, the average grain size of the pentacene films on both the ordered and disordered ODTS monolayers also increases. This morphological evolution is related to the activated surface diffusion process of the pentacene molecules according to the deposition kinetics.[15,19] The pentacene molecules preferentially diffuse on the surface as the substrate temperature increases, thereby being stabilized and captured in pentacene islands, which causes an increase in the pentacene grain size.

Figure 5 shows selected AFM topography images and height profiles of 30Å-thick pentacene films on ordered and disordered ODTS monolayers at various substrate temperatures. On the ordered monolayers (Figures 5a), laterally isotropic and flat pentacene domains are formed at all temperatures. The heights of the domains correspond to a thickness of about 2−3 layers considering the long axis of the pentacene molecule.[17] On the other hand, in the case of the disordered ODTS monolayers (Figures 5b), conglomerated island-type pentacene domains are observed; the heights of these domains were greater than those of the domains formed on the ordered monolayers. The height profiles shown in Figure 5 suggest that the conglomerated island-type pentacene domains have fewer crystal phases with their *(00l)* planes parallel to the dielectric surface than the laterally isotropic and flat ones. This results in a lower crystallinity of the pentacene films,[50–52,54] which is in agreement with the XRD results shown in Figure 2 and 3.

The output and transfer characteristics of devices with a channel length of 100 μm and a width of 800 μm are shown in Figure 6. All devices were found to be well-behaved p-type transistors with characteristics including a linear regime at small source-drain voltages (V_{DS}) and a saturation regime at V_{DS} values greater than the gate voltage (V_G) (Figure 6.a,c,e). The maximum

(48) Sato, T.; Yamada, Y.; Saijo, S.; Hori, T.; Hirose, R.; Tanaka, N.; Sazaki, G.; Nakajima, K.; Igarashi, N.; Tanaka, M.; Matsuura, Y. *Acta Crystallogr.* **2000**, *D56*, 1079.
(49) Venables, J. A.; Spiller, G. D. T.; Hanbücken, M. *Rep. Prog. Phys.* **1984**, *47*, 399.
(50) Dürr, A. C.; Nickel, B.; Sharma, V.; Täffner, U.; Dosch, H. *Thin Solid Films* **2006**, *503*, 127.
(51) Meyer zu Heringdorf, F.-J.; Reuter, M. C.; Tromp, R. M. *Appl. Phys. A: Mater. Sci. Process.* **2004**, *78*, 787.
(52) Zorba, S.; Shapir, Y.; Gao, Y. *Phys. Rev. B* **2006**, *74*, 245410.
(53) Zhang, Z.; Lagally, M. G. *Science* **1997**, *276*, 377.
(54) Cheng, H.-L.; Mai, Y.-S.; Chou, W.-Y.; Chang, L.-R.; Liang, X.-W. *Adv. Funct. Mater.* **2007**, *17*, 3639.
(55) Jang, Y.; Cho, J. H.; Kim, D. H.; Park, Y. D.; Hwang, M.; Cho, K. *Appl. Phys. Lett.* **2007**, *90*, 132104.
(56) Forrest, S. R.; Burrows, P. E. *Supramol. Sci.* **1997**, *4*, 127.
(57) Wang, H.; Zhu, F.; Yang, J.; Geng, Y.; Yan, D. *Adv. Mater.* **2007**, *19*, 2168.
(58) Eremthenko, M.; Schaefer, J. A.; Tautz, F. S. *Nature* **2003**, *425*, 602.

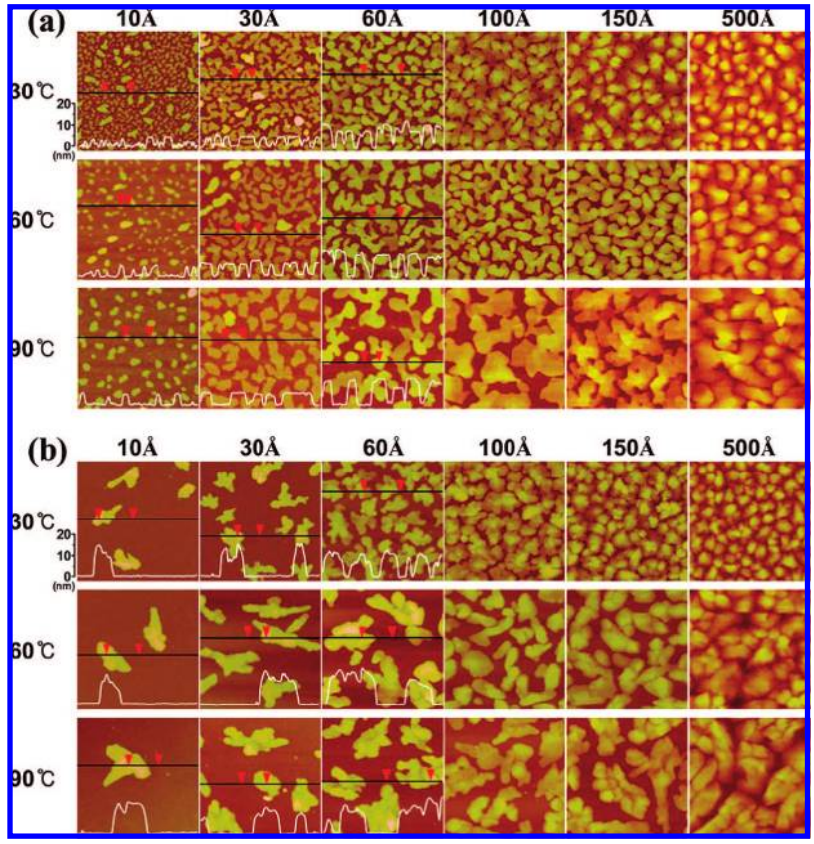

Figure 4. AFM images and height profiles taken at various thicknesses during the formation of pentacene films on ordered (a) and disordered (b) ODTS monolayers at substrate temperatures of 30, 60, and 90 °C. All images are 2 μm × 2 μm in size.

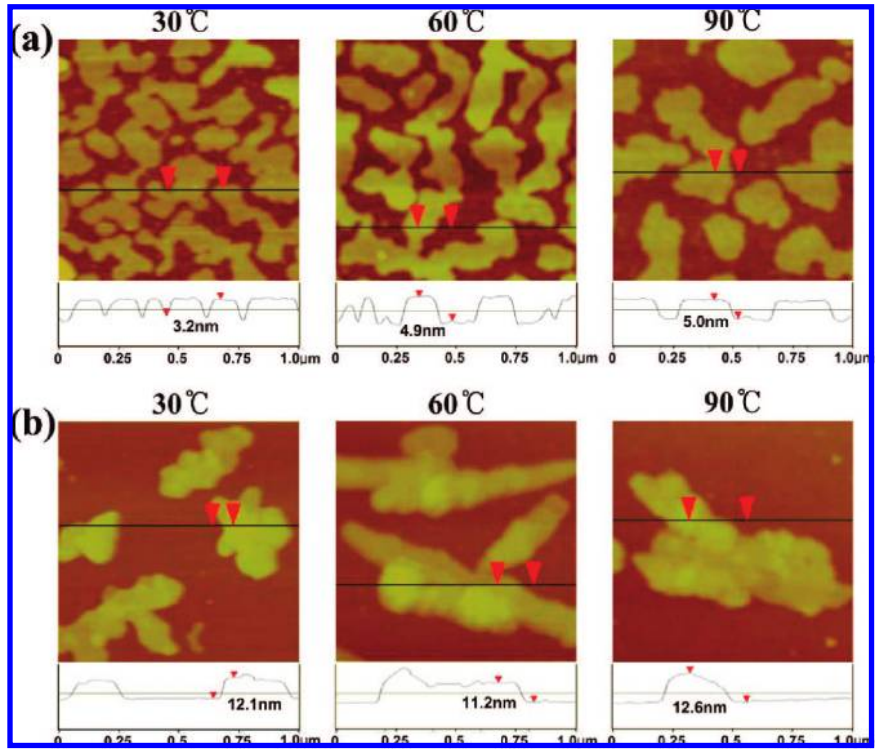

Figure 5. AFM images and height profiles of 30 Å-thick pentacene films deposited at 30, 60, and 90 °C on ordered (a) and disordered (b) ODTS monolayers. All images are 1 μm × 1 μm in size.

saturation currents at each V_G value were found to be higher by a factor of more than two for the devices fabricated using ordered ODTS monolayers than for those based on disordered ones. Furthermore, these currents were observed to increase

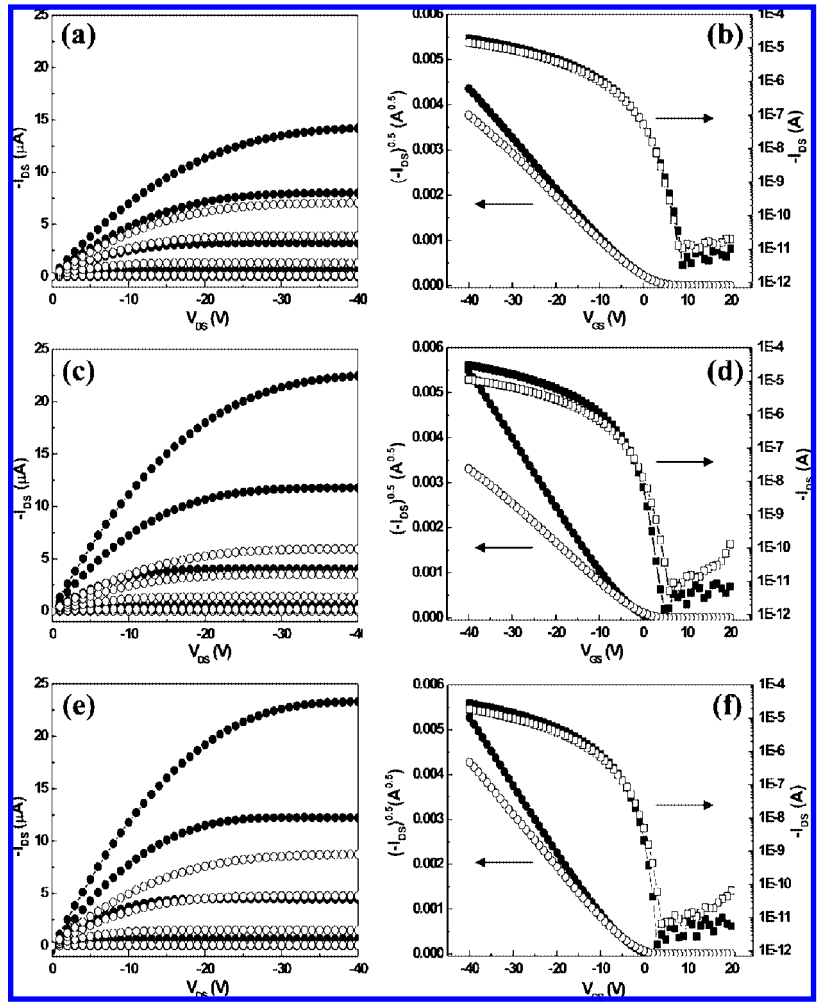

Figure 6. Electrical (output and transfer) characteristics of pentacene TFTs with the gate dielectric treated by ordered (closed symbols) and disordered (open symbols) ODTS monolayers. Substrate temperature: (a,b) 30 °C; (c,d) 60 °C; (e,f) 90 °C.

significantly with increasing substrate temperature in the case of the ordered-surface-based devices, a behavior that was not observed in the case of the disordered-surface-based devices. Figure 6 panels b, d, and f show the transfer characteristics as a function of V_G at $V_{DS} = -40$V. The on/off current ratios of all the devices were found to be above 10^6, independently of the substrate temperature. The carrier mobilities of the TFTs were calculated in this saturation regime—from a plot of the square root of the drain current versus V_G—by using the equation[55]

$$I_{Dsat} = \frac{\mu_p WC}{2L}(V_G - V_T)^2 \quad (1)$$

where W and L are the channel width and length, respectively, C is the capacitance of the gate insulator per unit of area, μ is the field-effect mobility, V_G is the gate bias, and V_T is the threshold voltage.

The mobilities of pentacene TFTs fabricated on ordered and disordered ODTS monolayers at various substrate temperatures are shown in Figure 7. It can be seen that the field-effect mobilities of the devices based on the pentacene films deposited on ordered monolayers are much higher. Furthermore, these mobilities were observed to increase significantly with increasing substrate temperature which did not happen in the case of the devices fabricated using disordered ODTS monolayers.

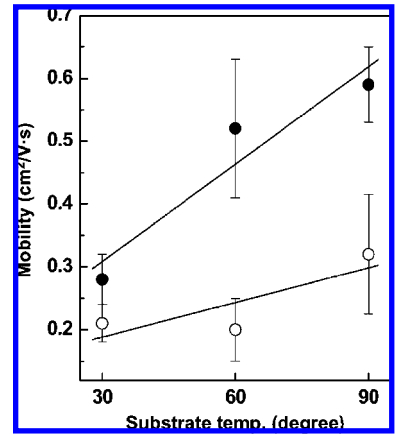

Figure 7. Field-effect mobilities of pentacene TFTs fabricated on ordered (closed symbols) and disordered (open symbols) ODTS monolayers at various substrate temperatures.

Before discussing the electrical properties of the TFTs, we would like to address the formation processes of the pentacene thin films on both types of monolayers. Quasi-epitaxy (QE) growth of the pentacene film on the ODTS monolayer may explain the differences in the growth mechanism and the crystallinity which are observed between the ordered and

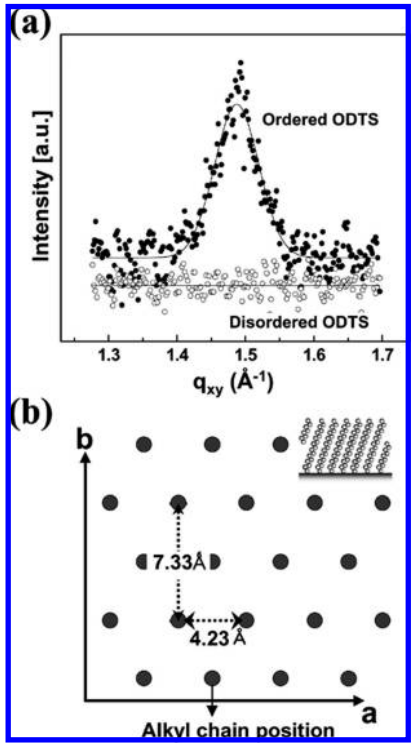

Figure 8. GI-XRD patterns of an ODTS monolayer (a) at a grazing angle of 0.18°. Schematic views of the in-plane lattice structures of the ordered ODTS monolayer (b).

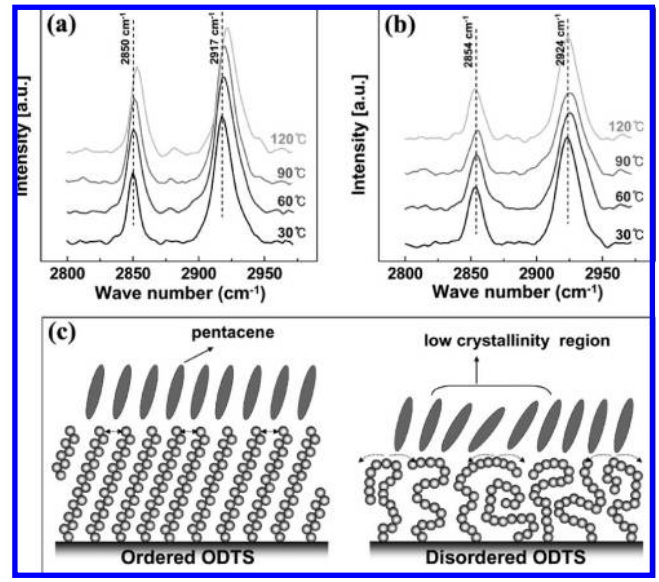

Figure 9. Infrared external reflection spectra of ordered (a) and disordered (b) ODTS monolayers on silicon showing the temperature dependent shifts of asymmetric and symmetric methylene (−CH_2−) stretching modes. (c) Schematic cross-section diagrams of the ordered and disordered ODTS monolayers and of the pentacene structures deposited on them.

disordered cases.[56,57] Usually, organic epitaxy refers to systems where the positions of the adlayer molecules are commensurate with the underlying substrate atomic or molecular positions.[56,58] In contrast, a QE is those in which the substrate and film are incommensurate over any meaningful lattice length scale. Despite this incommensurability, QE films can exhibit long-range order, and have a unique orientational relationship with the substrate lattice. QE growth can result in more stable strained structure than the bulk structure of the same material, by reduction of the strain energy in the internal lattice.[56–58] With the aim of clearly determining the lattice structure of ODTS monolayer, we also performed GI-XRD experiments. The data for ordered and disordered ODTS monolayers, prepared on a SiO_2 surface, are shown in Figure 8a. The peak observed at around 1.5 Å^{-1} in the ordered case could be assigned to the (10) diffraction of the hexagonal crystalline lattice, with a constant spacing of d_{10}= 4.23 Å for the alkyl-chain arrays (or a unit cell with the dimensions: a = 4.23 Å, b = 7.33 Å, and γ = 90°).[32,59–61] This diffraction peak was not observed in the disordered case. Figure 8b) shows a schematic representation of the in-plane lattice structure of the alkyl-chain arrays in the ordered ODTS monolayers. In consequence, by the interaction between the crystalline structure of the alkyl-chain array in the ordered ODTS monolayer and the pentacene molecules, the QE growth of the film may have occurred. On the other hand, no QE is observed in the case of the pentacene films deposited on the disordered monolayers, which is due to the amorphous state of the alkyl-chain arrays in the ODTS monolayer. This approach can explain the higher crystallinity and crystalline phase ratio (Figures 2 and 3) and 2D island growth (Figure 4) of the pentacene film on the ordered case, leading to a significant improvement of the carrier transport in organic devices.

The crystallinity increases remarkably with the substrate temperature in the ordered case, but only slightly in the disordered case (Figure 2). This difference in the degree of crystallinity may be a result of the different mobilities of the alkyl chains in both monolayers.[7,33,62,63] Figure 9 a and b show the FT-IR spectra of ordered and disordered ODTS monolayers as a function of temperature, respectively. For the ordered case [Figure 9a], peak frequency of both asymmetric (∼2917 cm^{-1}) and symmetric (∼2850 cm^{-1}) stretches for alkyl chain exhibited almost no shift with increasing temperature from 30 to 90 °C but a somewhat upward shift at 120 °C. These results indicate that the structure of alkyl chains is able to retain its ordering and uniformity in the tilt direction until around 90 °C by means of van der Waals interactions, and subsequently the orientation of them is collapsed at temperatures higher than 120 °C. On the other hand, for the disordered case (Figure 9b) prepared at 60 °C, the peak frequency shift is insensitive to any further increase in temperature. It is because the level of disorder in the alkyl chains is not greatly changed by "gauche defect saturation" effect with the increasing substrate temperature,[63] although random motion of the alkyl chains increases. On the basis of the results, we propose a schematic cross-sections of a pentacene monolayer deposited on ODTS monolayers with different alkyl-chain orientations in Figure 9c. In the case of the ordered monolayers, the surface of alkyl chains is relatively rigid, because they are strongly held together by means of van der Waals interactions. In contrast, the alkyl chains of the disordered monolayers are flexible due to the weak interactions between neighboring chains and the low chain packing density.[62,63] The mobility of the alkyl chains in the disordered

(59) Kojio, K.; Takahara, A.; Omote, K.; Kajiyama, T. *Langmuir* **2000**, *16*, 3932.
(60) Tinakata, T.; Imai, H.; Ozaki, M.; Saco, K. *J. Appl. Phys.* **1992**, *72*, 5220.
(61) Kojio, K.; Ge, S.; Takahara, A.; Kajiyama, T. *Langmuir* **1998**, *14*, 971.
(62) Lee, D. H.; Kim, D.; Oh, T.; Cho, K. *Langmuir* **2004**, *20*, 8124.
(63) Prathima, N.; Harini, M.; Rai, N.; Chandrashekara, R. H.; Ayappa, K. G.; Sampath, S.; Biswas, S. K. *Langmuir* **2005**, *21*, 2364.

case may assist the surface diffusion of the pentacene molecules, thus causing an increase in the grain sizes of the deposit.[7] This mobility may also affect the molecule-packing process in the pentacene grains (Figure 9c), which results in a low crystallinity of the pentacene films. As the substrate temperature increases, the alkyl chains in the disordered monolayers become much more mobile, which affects the crystallinity of the pentacene film. On the other hand, in the ordered case the mobility of the alkyl chains does not increase significantly due to their tightly packed structure. This is the reason why the crystallinity difference between the ordered and disordered cases increases with increasing deposition temperature (Figure 2).

Conclusions

To demonstrate the effect of the phase states of SAMs on both pentacene growth and the performance of pentacene-based TFTs, we used ODTS monolayers with different alkyl-chain orientations on the gate dielectrics. The pentacene films and devices based on ordered ODTS monolayers were found to exhibit a higher crystallinity and better electrical performance than those based on disordered monolayers. Furthermore, the differences between the field-effect mobilities of the pentacene films formed on both types of monolayers were found to increase with increasing substrate temperature. These results can be explained by (1) a quasi-epitaxy growth of the pentacene film on the ordered ODTS monolayer, and (2) different alkyl-chain mobilities resulting from the differences in the chain packing density and the chain orientation. Additional studies are needed to understand these phenomena and clarify the detailed mechanism.

Acknowledgment. This work was supported by a grant from Information Display R&D Center under the 21st Century Frontier R&D Program, ERC program (R11-2003-006-06004-0) of the MOST/KOSEF, the Regional Technology Innovation Program (RTI04-01-04), and POSTECH Core Research Program. The authors thank the Pohang Acceleratory Laboratory for providing the synchrotron radiation source at the 4B1, 4C2, 8A2, 8C1, and 10C1 beam lines used in this study.

Supporting Information Available: In-plane GI-XRD patterns; Rocking scans at (002) peak along out-of-plane of the 50 nm-thick pentacene films deposited on ordered and disordered ODTS monolayers. This material is available free of charge via the Internet at http://pubs.acs.org.

JA800142T